Kinematic Analysis of Cam Profiles Used in Compound Bows

A Thesis

Presented to

The Graduate Faculty of the University of Missouri

In Partial Fulfillment of the

Requirements for the Degree

Master of Science

Andrew Joseph Hanson

December 2009

The undersigned, appointed by the Dean of the Graduate School, have examined the thesis entitled:

KINEMATIC ANALYSIS OF CAM PROFILES USED IN COMPOUND BOWS

Presented by Andrew Joseph Hanson

A candidate for the degree of Master of Science

And hereby certify that in their opinion it is worthy of acceptance.

Professor Yuyi Lin

Professor Sherif El-Gizawy

Professor James Noble

ACKNOWLEDGEMENTS

To my advisor,
Yuyi Lin, Ph. D, P.E.,
for his amicable and devoted mentoring;

To my wife, Lauren,
for her patience and understanding;

And to God,
for His blessings each day.

ABSTRACT

The first compound bow was invented in Missouri in 1969. [Allen, 1968] Compound bows are uniquely different from other types of bows in that they use a set of cables, cams and pulley, and two elastic limbs that act as springs, to create a mechanical advantage while the bowstring is being drawn. In what is known as the let-off (draw force verses draw length) curve, this allows the archer to hold the bow at a fully drawn length with significantly less force than the maximum draw force. This design is advantageous for hunting, where arrow speed, accuracy, and holding weight become important requirements in being successful. Since the invention, technology has progressed in improving the bow's efficiency, accuracy, and arrow speed through patented empirical methods. However, very little has been shown in analytically modeling and optimal design of this complex mechanical system.

A preface to various types of bows as well as subtypes of compound bows will be introduced. A kinematic analysis will be shown for an eccentric-circular cam design and a one-cam one-pulley design. By iteratively determining the bow limb, cam, and cable positions a relationship between the drawn length and drawn force will produce a draw-force curve. In fact, this curve represents the strain energy stored within the system, and upon arrow release will be transferred into kinetic energy. Like all mechanical systems, there is a loss in energy and efficiency. A method for accurately determining efficiency will be explained. Experiments are also conducted using carbon fiber composites to create an adequate limb design.

TABLE OF CONTENTS

Page

LIST OF FIGURES

Figure Page

CHAPTER I

INTRODUCTION

1.1 – Types of Bows

The use of an archery bow dates back to prehistoric times, but as firearms began to replace bows as a military weapon in the 16th century, the bows' main purpose was for hunting and recreation. The archery bow can be classified into three categories: longbow, recurve bow, and compound bow.

The longbow is the oldest of the three types. Long bows consist of a D-shaped body that is connected to a string cable. The body on a long bow serves as a handle support and as an energy storing limb. Long bows measure approximately the height of a person. The longbow pictured in Fig.1 runs 78 inches in total length and has a pull force of 105 lbs at a 32 inch draw.

Figure 24 - Self-yew English Longbow, 6.5ft (www.wikipedia.org)

The draw length is measured from the handle position to the point the string connects to the arrow.

The second type of bow is the recurve. The recurve's drawstring, unlike the longbow, comes in contact with the bows limb as the string is being drawn. The contact between limb and string allows for a different relationship between the draw force and the length of the drawstring pulled. In general, the force is slightly less than linear as the archer reaches a fully drawn

position[Kincy, 1981]. Competition recurves run 20-50 lb and 62-70 inches in total length, hunting recurves run 40-60 lb and 58-62inches.

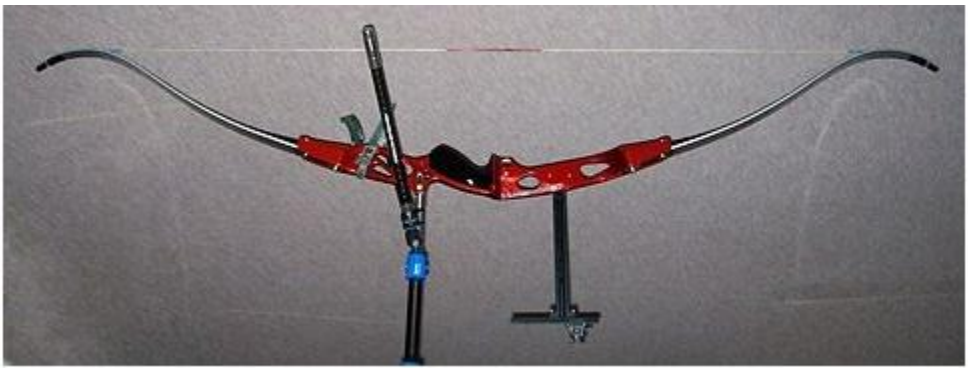

Figure 25 - Modern Recurve Bow (www.wikipedia.org)

The third type of bow, and the topic of this study, is the compound bow. The compound bow uses a cam or pulley pinned to the end of the limb along with a series of connected cables to provide a mechanical advantage allowing the bow to store more energy while requiring less force from the archer to hold the bow at a fully drawn position. Fig.3 is an

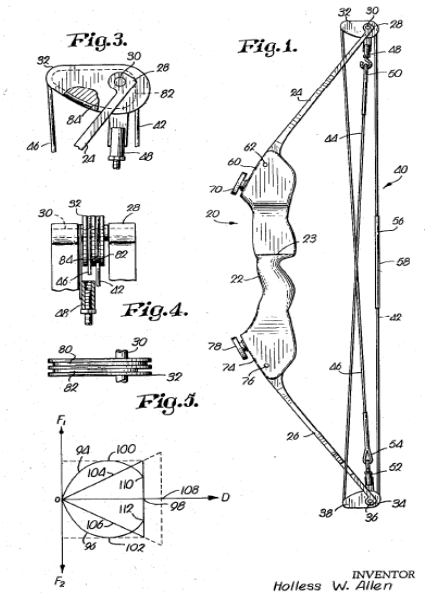

Figure 26 - First Compound Bow (US Patent 3486496)

example of the basic design of the first compound bow patented by Holless Allen in 1969. [Allen, 1969]

1.2 – Characteristics of a Compound Bow

The compound bow is a technologically more complex and advanced system that is uniquely different than the other two previous bow types. This system uses the limbs, like other bow types, to store energy to propel the arrow into motion. The bow's string cables are wrapped around the cams, and each cable performs a different function and carries a different load required to hold the limb in its deformed position. Refer to Fig.5 for an illustration of compound bow terminology. The bow cables consist of a draw string which is pulled by the archer and a set of buss cables that are on the non-draw side. In some cases one of the buss cables may be more accurately described as a controller cable. The distribution of force for each cable string is dependent upon the profiles of the cams. In general, as the cam rotates and the bowstring is drawn, the pull force (which is a function of the bowstring tension force) increases until it reaches a maximum draw force. Then, it begins to relax to a holding draw weight when the archer is in a fully drawn position. The relationship between the maximum draw force and the holding weight is known as let-off. The percentage let-off can be described as:

$$1-\frac{holdingweight}{\max weight}=letoff\times 100\% \qquad (1)$$

A let off curve is commonly shown to represent this relationship between the maximum draw force and holding force. The area under the curve, referring to Fig.4, is the amount of potential or strain energy that is stored in the limbs. Since the arrow is attached to the same position from which the archer pulls, the forces on the draw can be converted into kinetic energy that is

transferred to the arrow upon release. Not all strain energy stored in the limbs will be transferred into kinetic energy in the bow. In the market today a high-performance bow is around 80% efficient while some claim to be as high as 86-88% efficient. [www.huntersfriend.com, 2007]

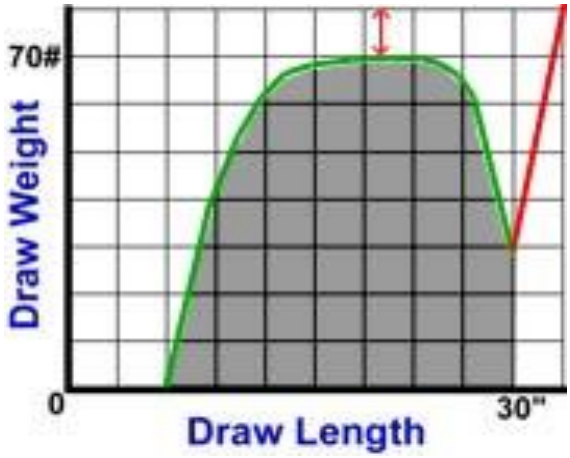

Figure 27 - Let-off Curve (www.huntersfriend.com)

Just a few years ago, the standard for a high end bow was to shoot arrows at a speed of 300 fps (feet/second). As bow designers continue to stride for greater efficiency by improving cam/limb designs, the high speed record of 300 fps has become a thing of the past. Although many hunters can shoot deer at 250 fps or less, the notion of being able to shoot faster arrows has given hunters a desire and interest to pay more for this technology, and also be able to hunt larger game.

For the purpose of being able to fairly compare one bow's speed to another, an IBO (International Bowhunting Organization) standard is established. IBO standards state that an arrow must weigh 5 grains per maximum draw force. [IBO Rules Class Definitions, 2009] Since hunting bows are tested at 70 lb maximum draw weight, the arrow must weigh 350 grains, or

0.8 ounces. Also, the draw length from handle to bow string must be 30 inches. Although it is not an IBO standard, most marketed bows have a let-off between 65-80 percent.

In Fig.5, a compound bow of the one-cam one-pulley design is illustrated. All compound bows consist of a riser, which acts as a platform to mount the limbs. The riser also contains a handle grip and an arrow shelf. The attached limbs are used like a spring to store energy. In their initial position the limbs are already pre-loaded. The bow's strings are categorized into a bow string and a set of buss cables which are on the draw side and non-draw side respectively. The cams contain a series of stacked cams (usually 2 or three depending on the design). In most

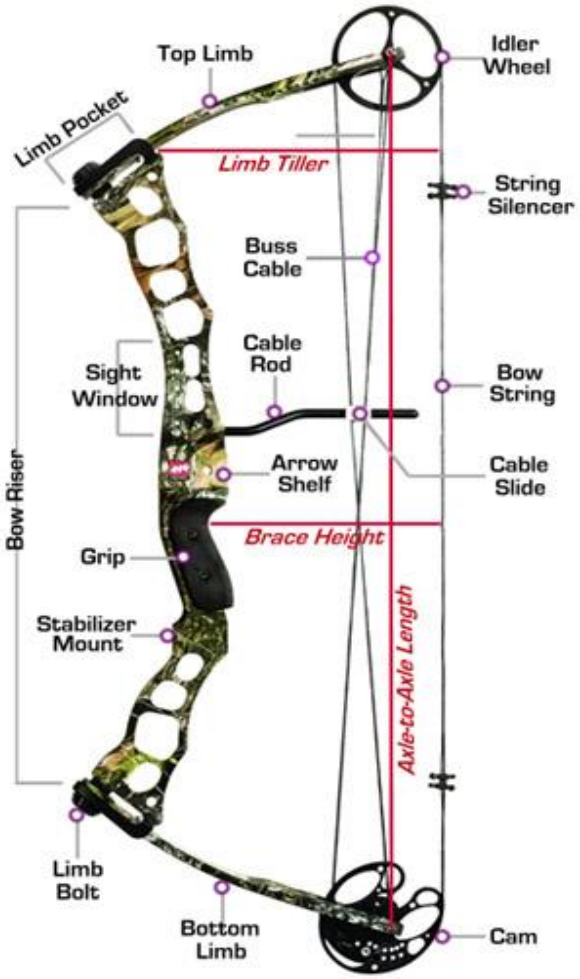

Figure 28 - Compound Bow Illustration (www.huntersfriend.com)

cases the bow string and buss cables are not physically connected (except on the pulley side of a single cam design). Although they are not connected, they are constrained to the cams rotation and usually end at some fixed location on the cam.

1.3 – Types of Compound Bows

Compound bows offer hunters a unique challenge that rifle hunting cannot offer. Compound bows require the hunter to get closer to their prey. Over the last few decades, many archery companies have been established to compete in this innovative industry. Within the branch of compound bows, there are four basic cam profile designs that are available on the market today. The four designs are the twin cam, hybrid cam, single cam and binary cam design. The website, www.huntersfriend.com, offers rich information in comparing these various designs. Each design offers its own set of advantages and disadvantages. For example, smoothness of draw, arrow speed, manufacturability, shooting accuracy, cost and so on.

A Twin Cam system is often considered a Two Cam or Dual Cam. The Twin Cam system contains two perfectly symmetrical round wheels or elliptical cams attached to the limbs. When properly synchronized, twin cams offer exceptional accuracy, nock travel, and overall arrow speed. A bow is said to have exceptional nock travel if the arrow's end attached to the string travels in a perfectly horizontal direction relative to the two limb ends. However, twin cams require more maintenance and service to stay in top shooting condition. Although it is desirable to have non-extensible strings, strings that do extend slightly have an effect on the synchronization of cam rotation. Twin cams also have a tendency to be noisier when shooting than hybrid or single cam designs. [www.huntersfriend.com, 2007] The first compound bow invention was of the twin cam design. Many youth bows, competition bows and serious shooters still prefer this design over some more expensive and technologically advanced

systems. Another advantage is eccentric circular cams are more easily manufacturable then some of the more complex cam.

The hybrid cam system has gained popularity over the last few years. The hybrid cam system features two asymmetrical elliptical cams: a control cam on top and a power cam on the bottom. The system is set up with a split-harness (buss cable), a control cable, and a draw string. Hybrid cams claim to offer the benefit of straight nock travel without synchronization issues. Although they are much more self reliant, they too need to be adjusted periodically to perform at their peak efficiency. There are several hybrid cam models that are impressively fast and

Figure 29 - Top Hybrid Cam (Controller Cam)

Figure 30 - Bottom Hybrid Cam (Power Cam)

quiet and can perform as good, if not better, than the even more modern single cam bows. Figs. 6 and 7 are an example of the hybrid cam system. In Figs. 6 and 7, although the draw side cams are symmetrical, the cam in its entirety is said to be asymmetrical. Therefore, it is not a twin-cam design. [www.huntersfriend.com, 2007]

The single cam system is often described as a Solocam or One Cam system with a round pulley wheel on the top and an elliptical shaped power-cam on the bottom. The single cam is generally quieter and simpler to maintain than traditional twin cam systems, since there is no need for synchronization of the top and bottom cam. US Patent 5,368,006 explains the single-

cams usefulness to solving previous synchronization issues. However, keeping nock travel straight becomes a more complicated tuning problem. Within a single cam system there is much room for variation allowing for some to have an aggressive let-off curve or a smoother draw. Some offer ease of adjustability, others do not. Overall, single cam reliability and smoothness is well respected and they are today's popular choice on compound bows. Fig.8 shows an example of a single cam which in all cases is connected to the bottom limb. It is sometimes called the power cam because it is responsible for the force distribution between cable strings. [www.huntersfriend.com, 2007]

Figure 31 - Bottom Single Cam (Power Cam)

Introduced in 2005 by Bowtech Archery, the binary cam is a modified 3-groove twin-cam system that constrains the top and bottom cam to each other, rather than to the bow's limbs. Fig.9 shows a binary cam. There are no split-harness connections to the limb on a binary system, like on a single or hybrid system, just cam-to-cam control cables. This creates a "free floating" system which allows the cams to automatically equalize any imbalances in limb deflection or string and control cable lengths. Although this design does not have much of a reputation in the

compound bow market, so far it has proven to shoot some of the fastest arrows. Those designs that were on the market in 2005 and 2006 were among some of the most popular. [www.huntersfriend.com, 2007]

Figure 32 - Binary Cam; No Split-harness Connection to Limb [www.bowtech.com,2009]

1.4 - Motivation

In this study, two separate cam systems are analyzed; the symmetric circular cam design (Chapter 2) and the one cam – one pulley design (Chapter 3). The modeled systems will yield a set of forcing vectors that will form a unity between the deformed limb, with a known spring constant, to the forces on the bowstring and buss cables. The purpose of this study is to analytically model the compound bow's system so that there is a greater understanding and ability to predict the effects of changes that are made to both the cam and limb characteristic geometry. With the following model equations, one can input a given cam profile and limb properties to accurately predict the draw-force curve thus allowing the theoretical arrow speed to be calculated. The goal is to create an accurate analytical approach to modeling a compound

bow's let-off, which can save both time and money that would be lost while making and testing design prototypes.

Chapter 4 will discuss experimental data for determining design efficiency, as well as a method for manufacturing bow limbs. One of the major marketing factors of compound bows is their ability to shoot fast arrows. Since most bows are 80% efficient, there is a considerable effort for improving the compound bow's efficiency.

1.5 – Literature Survey

There have been many advances in compound bow technology to date. Patents have improved the bow's efficiency and performance through empirical methods; however analytical methods were not evident. Theses have examined parts of the compound bow and some have even analyzed their draw-force relationship [Kincy, 1981; Visnor, 2007], but either the bows used were outdated or the assumed data was not accurate enough compared to actual physical characteristics of a compound bow.

The first patented compound bow was of the symmetric cam type. [Allen, 1968] At that time, using eccentric discs to create a mechanical advantage was very different than the traditional long bow and even the recurve bow. In 1977, Kudlacek invented the bow that used eccentric cam elements. This design is still in production today on some of the more basic hunting bows and youth bows for the simplicity of manufacturing circular discs. Chapter two is devoted to analyzing this type of bow, because it is a good starting point for understanding how the cam and limb geometry affect the let-off curve.

A one cam – one pulley (single cam) design was first patented in 1994 by McPherson and as of 2006 accounted for 46% of compound bow sales. [huntersfriend.com, 2007] The design uses

a pulley on the upper end and an eccentric layer of cams on the lower end. The purpose of the stacked cams is to approximately feed the same amount of string out the pull side and tie the two limbs together during its draw. One advantage of this type of design is that adjusted draw lengths can be achieved using the same string while nock travel is unaffected.

Progresses have been made for increasing maximum stored energy, bow efficiency, and usability to improve the single-cam bow. In Darlington's patent [2000] an adjustment allowed a flatter contour to be maintained at the maximum force/draw curve for adjustable draw lengths. Strother's patented design [2007] claims 82-94% efficiency can be achieved using his single-cam design; however, others claimed that the best tested bows have not performed over 88%. Another patent allows for the buss cable to act through the axel pin achieving nearly 100% let-off on the drawn bowstring. [Blahnik, 2006; Knittel, 2008] Chapter 3 is devoted to modeling a one cam – one pulley design.

A thesis [Kincy, 1981] was presented to the University of Missouri – Rolla which used a method to iteratively model the limb, string, and eccentric wheel mechanics. The compound bow being modeled was a patented [Ketchum, 1976] bow. The thesis used Bernoulli – Euler's equation for bending. The cantilever beam segment was iteratively broken into segments and the force required to bend the beam was distributed among the bow's cable strings by summing the torques about a central point on the beam segment. In the thesis, however, it did not explain how to improve the strain energy storage.

A more recent thesis explains in detail the limb deflection of a cantilever beam under large deflection as related to a compound bow. [Visnor, 2007] Visnor's thesis explains an analytical approach to accurately determine the limb tip position of a beam subjected to a constant, concentrated force, with a constant angle applied to the free end. However, realistic

characteristics of a bow will not have a constant force, since the limb tip is changing location, and the angle the force applied will change as well.

CHAPTER 2

ANALYSIS OF A SYMMETRIC CIRCULAR CAM DESIGN

2.1 – Introduction to Symmetric Circular Cam Analysis

As a good starting point for analyzing translation and rotation of a cam on a limb, first a twin eccentric cam design is considered. In this type of design, there are assumptions that can be made to simplify the analysis process. This type of design has two completely symmetrical cams which rotate in unison and likewise both the top and bottom limbs will deform concurrently. We can also assume the riser to be completely rigid and the strings to be inextensible. To solve this problem we will set up a global coordinate system with a center at the mid-point of the riser. This point is where the arrow rests on the riser.

Referring to Figs.11 and 12, our objective is to solve for the tangent point, (X_t^i, Y_t^i), connecting the cam to the bowstring and buss cable as well as correctly determine the exact global coordinate position of (X_c^i, Y_c^i). This can be done by using a cam rotation of θ_i as an input where *i* =1 to n. By knowing the exact location of (X_c^i, Y_c^i) the limb deformation is known as well. After calculating the buss cable side the bow string side will be determined. If we assume the limbs to be cantilever beams with known physical properties, then their spring force is known as well. A moment about point (X_c^i, Y_c^i) and the distance to the bow string and buss cable create a ratio that will become important in calculating the amount of force on each string.

$$F_{bowstring}\, M1 = F_{busscable}\, M2 \qquad (2)$$

In Equation 2, $F_{bowstring}$ is the tension force on the bow string, $F_{busscable}$ is the tension force on the buss cable and M1 and M2 are the distances previously mentioned from (Xc,Yc) to their respective strings.

2.2 – Determining a Point on an Eccentric Circle

Let us next look at the geometry of a circle with an offset center shown in Fig.10. We can determine the points (X_p^i, Y_p^i) for a rotation, θ_i, about the center (X_c, Y_c) using the circle and slope equations.

$$R^2 = (X_p{}^i)^2 + (Y_p{}^i)^2 \qquad (3)$$

$$\frac{Y_p^{\,i} - Y_c^{\,i}}{X_p^{\,i} - X_c^{\,i}} = \tan(\theta_i) \qquad (4)$$

R is the known geometric radius of the cam. The points X_c and Y_c are assumed to be known using a set of equations discussed later on. So, for an incremental rotation, θ we can find the points on the circle, X_p and Y_p.

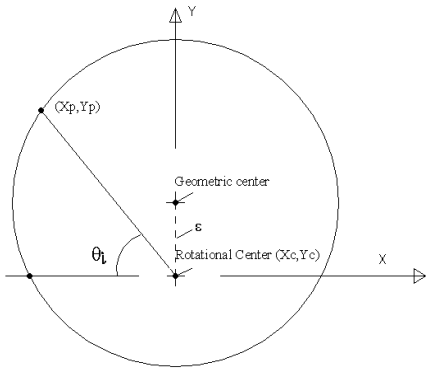

Figure 33 - Circle Geometry Used to Calculate (Xp,Yp)

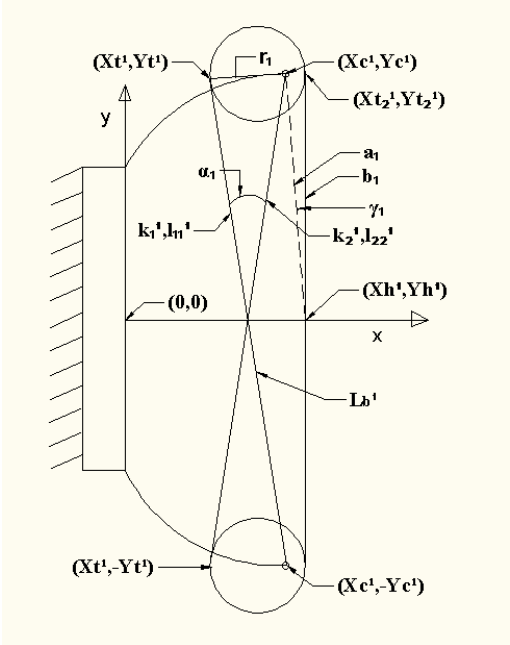

Figure 34 – Eccentric Cam Bow in First Iteration

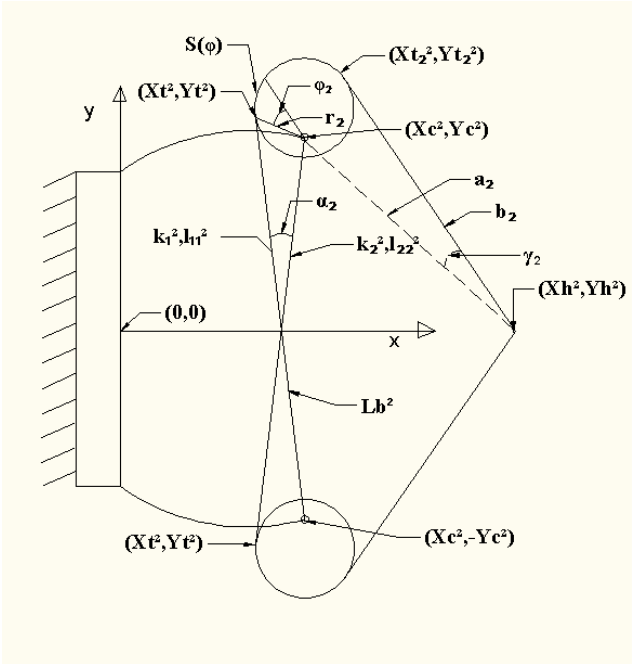

Figure 35 – Eccentric Cam Bow in Second Iteration

2.3 – Geometry Analysis for Determining Tangent Points

Continuing on in our discussion, we will refer to Figs. 11 and 12 to formulate a set of equations that will allow us to solve our new geometry for a given cam rotation θ. Fig.11 represents the initial conditions of the compound bow and Fig.12 can be considered one angle of rotation θ. (X_t^i, Y_t^i) are coordinate positions for the tangent point of the buss string connected to the non-draw stacked cam. (X_c^i, Y_c^i) likewise are coordinate positions of the cams center of rotation and will be the same for both the draw and non-draw side cams. Since the bow is modeled symmetrically about the x-axis, which is the arrow's draw plane, we can say that the other cam will have a tangent point $(X_t^i, -Y_t^i)$ and a center location of $(X_c^i, -Y_c^i)$. Variable L_b^i represents the length of the string from the connection on the limb to the tangent point on the cam and k_1^i and k_2^i represent their slopes respectively. L_b^i will be the same for both buss cables due to symmetry. Variable r_i will represent the radial distance from the center of rotation to the tangent point on the cam and angle α_i is between l_{11}^i and l_{22}^i. It can be solved using the slope of k_1^i and k_2^i. Also, ϕ will be the angle created by the first tangent point to the i^{th} tangent point. All initial conditions can be assumed to be known.

For Fig.12 we wish to know the coordinate position of (X_t^i, Y_t^i), (X_c^i, Y_c^i), k_1^i and k_2^i from a rotation and forced translation. Equations 5, 7, 8, 12 and 15 can be used to solve for (X_t^i, Y_t^i), (X_c^i, Y_c^i), k_1^i and k_2^i. The first is the length of the string L_B.

$$L_B = S_\phi + \sqrt{(X_t^{\,i} - X_c^{\,i})^2 + (Y_t^{\,i} + Y_c^{\,i})^2} \qquad (5)$$

$$S_\phi = \int_0^\phi r(\phi)\, d\phi \qquad (6)$$

S_ϕ is the distance of string rolled onto the cam. Keep in mind that the shape of the cam will cause the tangent point to change; therefore θ will not necessarily equal ϕ. Also, *r(*θ*)* can be related to a coordinate translation and rotation. The second equation is the slope of the string connected to the top cam and the third is the slope of the string connected to the bottom cam.

$$\frac{Y_t^{\,i} + Y_c^{\,i}}{X_t^{\,i} - X_c^{\,i}} = k_1^{\,i} \qquad (7)$$

$$\frac{Y_c^{\,i} - Y_t^{\,i}}{X_c^{\,i} - X_t^{\,i}} = k_2^{\,i} \qquad (8)$$

The fourth equation (Equation 12) uses the law of cosines to make a relationship between the triangular sides l_{11}^{i}, l_{22}^{i} and r_i.

$$l_{11}^{i} = \sqrt{(Y_t^{i})^2 + (X_t^{i} - X_0^{i})^2} \quad (9)$$

$$l_{22}^{i} = \sqrt{(Y_c^{i})^2 + (X_c^{i} - X_0^{i})^2} \quad (10)$$

$$X_o^{i} = k_1^{i} X_t^{i} + Y_t^{i} \quad (11)$$

$$r_i^{2} = (l_{11}^{i})^2 + (l_{22}^{i})^2 - 2(l_{11}^{i})(l_{22}^{i})\cos\alpha \quad (12)$$

X_0^{i} is the X-location when Y=0 used to solve distances l_{11}^{i} and l_{22}^{i}. Distance r_i will need to be determined from points (X_t^{i},Y_t^{i}) and (X_c^{i},Y_c^{i}), where:

$$r_i = \sqrt{(X_t - X_c)^2 + (Y_t - Y_c)^2} \quad (13)$$

The last equation can be determined by finding a local curve of the cam profile. This can be accurately determined if we use least squares fitting using seven points from the cam geometry calculated in Equations 3 and 4. The seven points that are used will include: $[(X_p^{i},Y_p^{i}),(X_p^{i+1},Y_p^{i+1}), \ldots (X_p^{i+7},Y_p^{i+7})]$. Once there is an equation for the top cam, it can be made in the quadratic form:

$$ax^2 + bx + c = 0 \quad (14)$$

Where *a, b,* and *c* are determined constants. If we take the derivative of the previous equation and evaluate it at (X_t^{i},Y_t^{i}) it should equal the slope k_1^{i}.

$$k_1^{i} = 2(aX_t^{i}) + b \quad (15)$$

Likewise, seven points for the bottom cam, $[(X_p^{i},-Y_p^{i}),(X_p^{i+1},-Y_p^{i+1}), \ldots (X_p^{i+7},-Y_p^{i+7})]$, can be used to make a quadratic equation using least squares fitting. If the derivative is evaluated at $(X_t^{i},-Y_t^{i})$, an equation for k_2^{i} can be found similar to Equation 15.

The tangent point connected to the bowstring needs to be determined as well. Note, although in Figs. 11 and 12 there is only one circle, in reality there will be two eccentric stacked cams with different geometries and starting points, (X_p^{1},Y_p^{1}). This can be done using a similar set

of equations to those used in calculating the tangent point and rotational center on the buss cable side of the bow. We will again refer to Figs. 11 and 12 to find (X_{t2},Y_{t2}), and X_h. Y_h is considered to be along the X-axis, therefore it is zero. Three equations will need to be solved for these three unknown variables. Similar to Equations 7 and 8:

$$k_b^{\,i} = \frac{Y_{t2}^{\,i}}{X_{t2}^{\,i} - X_h^{\,i}} \tag{16}$$

$$k_a^{\,i} = \frac{-Y_{t2}^{\,i}}{X_{t2}^{\,i} - X_h^{\,i}} \tag{17}$$

where $k_a^{\,i}$ and $k_b^{\,i}$ are the slopes of lines a_i and b_i. $k_b^{\,i}$ is calculated from the derivative of the local cam curve from the top cam determined at the tangent point $X_{t2}^{\,i}$. The curve can be found by inputting the next seven points, [($X_{p2}^{\,i}$,$Y_{p2}^{\,i}$),($X_{p2}^{\,i+1}$,$Y_{p2}^{\,i+1}$), … ($X_{p2}^{\,i+7}$,$Y_{p2}^{\,i+7}$)], for the draw side of the top cam into the least squares fitting formula. $k_b^{\,i}$, likewise, can be found using the bottom cam on the draw side and least squares fitting. Equation 21 uses the law of cosines to create a triangle with side's a_i, b_i and c_i. Where c_i is the distance between ($X_{t2}^{\,i}$,$Y_{t2}^{\,i}$) and ($X_c^{\,i}$,$Y_c^{\,i}$). Side's a_i and b_i are shown in Figs. 11 and 12.

$$a_i = \sqrt{(Y_{t2}^{\,i})^2 + (X_c^{\,i} - X_h^{\,i})^2} \tag{18}$$

$$b_i = \sqrt{(Y_{t2}^{\,i})^2 + (X_{t2}^{\,i} - X_h^{\,i})^2} \tag{19}$$

$$c_i = \sqrt{(Y_{t2}^{\,i} - Y^i{}_c)^2 + (X_{t2}^{\,i} - X_c^{\,i})^2} \tag{20}$$

$$c_i^{\,2} = a_i^{\,2} + b_i^{\,2} - 2a_i b_i \cos(\gamma) \tag{21}$$

γ represents the angle between a_i and b_i. Once X_h reaches its maximum desired draw length the calculations stop.

2.4 – Force Discussion

In Chapter 3, a more extensive force analysis will be performed to solve the draw force for all iterations. In this case, symmetry will allow us to analyze the top cam only. Since all geometry

points are known at this time, an equation for torque can be applied to one side of the bow to find a ratio of the forces on the cam. The moment distances can be solved as the distance from (Xc,Yc) to the cable while staying perpendicular to the cable. The ratio between the two distances creates a ratio between the two forces (see Equation 2). This ratio will allow us to find the direction formed by the combination of forces connected to the cam, since the direction of each individual force is known. Likewise, the direction of the cable connected to (Xc,Yc) is known from our previous analysis. If we assume the spring constant is known for the limb, the magnitude of the limb can be determined. The direction of the limb force can be assumed to be opposite the path of the limb travel, where the limb travel is in the direction of the last cam center to the current cam center for all iterations. A forcing vector for all of the acting forces must be equal to zero. Since we know the magnitude and direction of the limb force and the direction of the combined forces connected to the cam in addition to the direction of the cable force through the center, the magnitude of the combined forces and the direction of the cable force through the cam center can be determined. Once the combined forces magnitude is known, each individual force can be solved by knowing the ratio that was already determined between these forces. The magnitude of the drawstring will allow us to find the magnitude of the draw force for all iterations. Equation 22 gives the relationship between the draw force and the force on the bowstring, where θ is the angle of the bowstring to the x-axis.

$$F_{string} = \frac{F_{draw}}{2\cos\theta} \qquad (22)$$

CHAPTER 3

ANAYLSIS OF ONE CAM – ONE PULLEY DESIGN

3.1 – Analytical Model

A generalized one cam – one pulley design holds a set of two strings that are wrapped around three cams that are stacked as shown in Figs. 13 and 14. C1, C2 and C3 are in reference to the three stacked cams. For a right handed draw, C1 is on the left side and is connected to the bowstring which also wraps around the pulley and connects to C3 (the right most cam) on the non-draw side. The middle cam, C2, contains the controller cable, since the cable is connected to the limb and controls the amount of travel of the limb tip. For the analysis of one cam – one pulley design we will assume that both limbs deform equally and the limb deforms linearly since the travel distance is relatively small. Also noted in Fig.13, (0,Yh) represents the bowstring nock point connected to the arrow. The nock point, Yh, is along the y-axis. (Xp,Yp) represent the

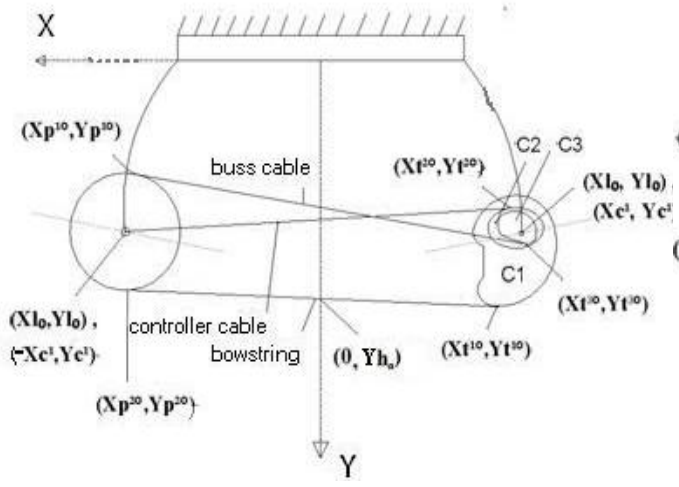

Figure 36 - One-Cam One Pulley, First Iteration

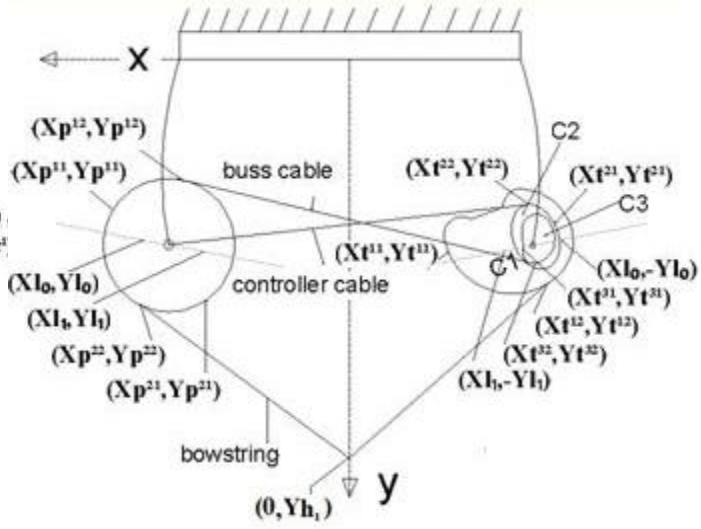

Figure 37 - One-Cam One Pulley, Second Iteration

tangent point connecting the string to the circular disk. For the first superscript, 1 denotes the non-draw side and 2 denotes the draw side. The second superscript denotes the iteration number. (Xl,Yl) is the measured limb tip in the (X,Y) coordinate system. (Xl_0,Yl_0) is the first iteration, and (Xl_1,Yl_1) is the last iteration. The line formed between these two points is the path of (Xc,Yc) travel. (Xc,Yc) is the rotational center of the pulley with the superscript denoting the iteration. Likewise, (-Xl,Yl) and (-Xc,Yc) represent the rotational center of the cam. (Xt,Yt)

represent the tangent points on the cam. The first superscript denotes the cam; C1, C2 and C3. The second superscript denotes the iteration. In Fig.14, there are sub-iterations for (Xp,Yp) and (Xt, Yt). The first would correspond to a translation and the second to a rotation. Therefore, for every (Xc,Yc) and (0,Yh) iteration, there are two (Xp,Yp) and (Xt,Yt) sub-iterations. Note, in Figs.13 and 14 the illustration is rotated 90 degrees clockwise in relation to Figs.11 and 12 so that a local curve can be formed near (Xt,Yt) for cams C1, C2 and C3. The importance will be seen later on in the discussion.

For analyzing the kinematics of the system the following assumptions must be made. The first is that there is no slippage of cable on the cams or pulley. Second, the string is inextensible. Third, the string is considered to be taut. Fourth, as previously mentioned, the limbs deform linearly and evenly. The top and bottom limb deform the same for all iterations. And finally, we assume to know the geometry of the pulley, cams, and limb. The measured cam geometry is taken from the rotational axis of C1, C2 and C3 to the edge of the cam. The first point taken is the tangent point of the given cam being measured. Then, an appropriate step size is chosen to allow for accurate results. A reference angle between C1, C2 and C3 must be measured. See Appendix E – Buckmaster BTR Measured Cam Profile for an example of measured data. By knowing the geometry of the limb and its material properties, a close approximation of the spring force of the limb can be determined. After kinematically determining the position of (Xc,Yc), Yh, both (Xp,Yp)'s and all (Xt,Yt)'s, a forcing vector between all the strings under tension can be created to find the amount of force required to pull Yh along the y-axis. This will yield the desired let-off curve for the given bow system.

To analyze the system, it can be broken into three sub-routines. All three routines will use the string length as the constraining factor. The input will be the limb deflection. For the first sub-routine, we will analyze the length of the controller cable, CC, connected to the controller cam, C2, and the upper limb. Since CC is connected to the upper limb, we know (Xc, Yc) for all iterations. The total length of the string will include the length from the upper limb tip to the tangent point on C2, L_2, in addition to the amount of string wrapped on C2, S_2. The total length of CC will remain constant for all iterations. The cam must be rotated until Equation 30 is satisfied.

$$CC = L_2 + S_2 \tag{23}$$

$$L_2 = \sqrt{(Yc^i - Yt^{2i})^2 + (Xc^i - Xt^{2i})^2} \quad (24)$$

$$S_2 = \int_{i-1}^{i} \sqrt{1 + \left(f(x)'\right)^2}\, dx \quad (25)$$

In Equation 24, L_2 is the length of the string from the center of rotation on the upper limb to the tangent point on C2. In Equation 25, S_2 is the length of cable wrapped on C2. S_2 can be determined from the measured cam data. The function, *f(x),* is found using least squares fitting similar to chapter 2. For all rotations, an arbitrary number of data points, for which the cam will be rotating onto, should be chosen to find a local curve that accurately represents the cam profile. Note that the data is in reference to the center of rotation. For Equation 25, *i-1* represents the last iteration tangent point after translation and rotation on C2. *i* represents the current tangent point.

It is important to determine the amount of rotation so that Equation 23 is satisfied. To satisfy Equation 23 we must find the tangent point (Xt^2,Yt^2) for each rotation. The tangent point can be found using the slope equation and the derivative of the local curve, *f(x)*.

$$\frac{Y_c^{\,i} - Y_t^{\,2i}}{X_c^{\,i} - X_t^{\,2i}} = K_2 \quad (26)$$

$$f(x) = aX^2 + bX + c$$
$$f(x)' = 2aX + b \quad (27)$$

$$K_2 = 2aX_t^{\,2i} + b \quad (28)$$

By solving Equations 26 and 28, we have the tangent point Xt^{2i}. Equation 26 is the slope equation through (Xc,Yc) and (Xt^{2i},Yt^{2i}), and Equation 28 is the slope of C2 at Xt^{2i}. *a* and *b* are determined coefficients using least squares fitting. By substituting the first part of Equation 34 in for Yt^{2i} evaluated at Xt^{2i}, the two unknowns are Xt^{2i} and K_2.

Once the tangent point is found, Equations 24 and 25 can be solved. If the rotation satisfies Equation 23, then the subroutine is complete. If not, the cam must be rotated more or less. The amount C2 rotates is directly related to the value, CC. CC must have an acceptable convergence

in order to continue. The rotation of C2 will be designated as σ. Since C1, C2 and C3 are a rigid body, σ will be the same.

Next, the second sub-routine will be performed to determine the tangent point of C3 (Xt^3,Yt^3) and the tangent point of the pulley on the non-draw side (Xp^1,Yp^1) for all iterations. There will be four constraining equations and four unknowns that need to be solved simultaneously. Like the first sub-routine, we will find a local curve of C3 after rotation. The function, *f(x)*, using least squares fitting, will again take the following form:

$$f(x) = aX^2 + bX + c. \qquad (29)$$

Note that *f(x)*, in this case, is for the local cam curve, C3, and the coefficients will be uniquely different. By taking the derivative of this function, and evaluating it at Xt^{3i}, the first equation can be formed to determine the slope of the buss cable, where K_3 represents the slope.

$$K_3 = 2aX_t^{3i} + b \qquad (30)$$

The second equation,

$$K_3 = \frac{Y_p^{1i} - Y_t^{3i}}{X_p^{1i} - X_t^{3i}}, \qquad (31)$$

is the slope equation from the tangent point on the pulley to the tangent point on C3. The third equation is the equation for the circular pulley with a radius, *r*.

$$(X_p^{1i} - X_c^{i})^2 + (Y_p^{1i} - Y_c^{i})^2 = r^2 \qquad (32)$$

The last equation can be formed since the tangent point (Xp^1,Yp^1) must create a 90 degree intersection between the slope of the buss cable and the slope from the pulley's center. Therefore,

$$K_3 = -\left(\frac{Y_p^{1i} - Y_c^{i}}{X_p^{1i} - X_c^{i}}\right)^{-1} \qquad (33)$$

If Equations 30-33 are solved simultaneously, and for Equation 29, $a(Xt^{3i})^2+b(Xt^{3i})+c= Yt^{3i}$, the four unknown variables become Xp^{1i}, Yp^{1i}, Xt^{3i}, and K_3.

To determine the rotation, ϕ, of the pulley after an input translation, the length of the inextensible buss cable will be considered. The following equation for the length of the buss cable, *BC*, will be used:

$$BC = S_{3i} + L_{3i} + S_{p1i} \tag{34}$$

where S_{3i} is the length wrapped on C3, L_{3i} is the length of the buss cable from the tangent point (Xt^{3i},Yt^{3i}) to the tangent point (Xp^{1i},Yp^{1i}), and S_{p1i} is the length of string wrapped on the non-draw side of the pulley. The length, BC, is assumed to be constant. S_{30} (initial length) will have its largest value, and can be measured. As the cam rotates C3 lets out string. S_{3i} can be calculated by the change in arc length. By using Equation 25, where *i-1* is the previous tangent point, *i* is current tangent, and *f(x)* is local curve function that is calculated using least squares fitting for C3, the change in S_3 can be determined. The original value, S_{30}, subtract the change in S_3 yields S_{3i}. Note the change in S_3 must be added to the accumulative change on C3. L_{3i} is found using the previously known values from calculating Equations 30-33 and the following equation.

$$L_{3i} = \sqrt{(Y_p^{1i} - Y_t^{3i})^2 + (X_p^{1i} - X_t^{3i})^2} \tag{35}$$

Using Equation 36, we can solve for S_{p1i} to find the rotation angle, ϕ, of the pulley. In Equation 36, *r* is the radius of the pulley.

$$\phi = \frac{S_{p1i}}{r}. \tag{36}$$

In the final sub-routine, the nock point, Yh, must be found. Since we assume Yh to be drawn linearly along the y-axis, the point can be found considering the length of the string from the y-axis to the tangent point on the bowstring side of the pulley. The initial length, L_{40}, can be determined from measurement. It is:

$$L_{40} = \sqrt{(X_p^{20} - X_{h0})^2 + (Y_p^{20})^2}\ . \tag{37}$$

Since we know the rotation that is required of the pulley due to the constraint of C3 and the buss cable length, we can determine the additional length that is added to BS_4; the total length from (Xp^2,Yp^2) to Yh for all iterations. There is an additional length, S_{p2i}, that must be add to BS_4

to account for the change in the string angle, γ, from the y-axis. Therefore, the amount of additional string is:

$$S_{p2i} = r(\phi + \Delta\gamma). \quad (38)$$

In Equation 39, $\Delta\gamma$ represents the change in the drawstring angle, where

$$\Delta\gamma = \gamma_i - \gamma_{i-1} \quad . \quad (39)$$

From Equation 37 and 38, BS_4 becomes,

$$BS_{4i} = \sqrt{(X_p^{2(i-1)} - X_{h(i-1)})^2 + (Y_p^{2(i-1)})^2} + r(\phi + \Delta\gamma) \quad (40)$$

Equation 40 introduces a few other unknowns that must be found in order to solve for Xh. The above unknowns are (Xp^2,Yp^2) and γ. Equations 41-43 are used in conjunction with 40 to solve these four unknowns: Yh, Xp^2, Yp^2, and γ for all iterations.

$$X_p^{2i} = X_c^i + r\cos\left(\frac{\pi}{2} + \gamma\right) \quad (41)$$

$$Y_p^{2i} = Y_c^i + r\sin\left(\frac{\pi}{2} + \gamma\right) \quad (42)$$

$$\gamma = \cos^{-1}\left(\frac{(Y_{hi} - Y_{h0})^2 + \left(Y_p^{2i} - Y_{hi}\right)^2 + \left(X_p^{2i}\right)^2 - \left(\left(Y_p^{2i} - Y_{h0}\right)^2 + \left(X_p^{2i}\right)^2\right)}{2\sqrt{\left(Y_p^{2i} - Y_{hi}\right)^2 + \left(X_p^{2i}\right)^2}\left(Y_{hi} - Y_{h0}\right)}\right) \quad (43)$$

Yh can also be solved from the cam side of the bow. To get a more accurate Yh, the mean of the two values will be used. If the Yh found on the pulley side and the Yh found on the C1 side is relatively far apart, then it is a good indication that the design needs improvement. To find Yh we will assume that the bowstring is disconnected at the draw axis. To find Yh, we will also need to know the tangent point (Xt^1,Yt^1) and the slope, K_1, of the bowstring for all iterations. First, a local curve using least squares fitting, similar to Equation 29, must be found after translation of C1. If the derivative of the equation, *f(x),* is evaluated at the tangent point (Xt^{1i},Yt^{1i}) the first equation becomes:

$$K_1 = 2aX_t^{1i} + b. \qquad (44)$$

The second equation is the slope of the line from Xh to the tangent point (Xp^1,Yp^1).

$$K_1 = \frac{Y_{hi} - Y_t^{1i}}{-X_t^{1i}} \qquad (45)$$

The third equation is the length of the bowstring from Xh to (Xp^{1i},Yp^{1i}). The length of the bowstring is the initial length in addition to the amount of string that has been unwrapped. Equation 46 can be written as:

$$\int_0^i \sqrt{1+\left(f(x)'\right)^2} + \sqrt{\left(X_{h0} - X_t^{10}\right)^2 + \left(Y_t^{10}\right)^2} = \sqrt{\left(X_{hi} - X_t^{1i}\right)^2 + \left(Y_t^{1i}\right)^2} \qquad (46)$$

The unwrapped length is evaluated from the initial tangent point to the current tangent point. If the local curve is used, we can substitute Yt^{1i} for $a(Xt^{1i})^2+b(Xt^{1i})+c$. This will reduce the number of unknown variables and equations that are needed, and allow us to solve for Xhi, Xt^{1i} and Yt^{1i} using Equations 44-46.

3.2 – Force Analysis

The objective of determining the tangent points is a key part to solving the draw force for all iterations. This will allow the directions of each force connected to a cable to be known In Fig.15, the force directions F1, F2, F3, F4, F5, F6, Fspring, and Fdraw are depicted. Fspring may not act along the direction the limb tip travels. Although not shown, T1, T2,T3, T4, T5, and T6 are the torques created by the forces F1, F2, F3, F4, F5, and F6 respectively multiplied by their moment distances D1, D2, D3, D4, D5, and D6 respectively about the cam center of rotation. For Fig.15, the forces are not drawn to scale, but are descriptive of their direction.

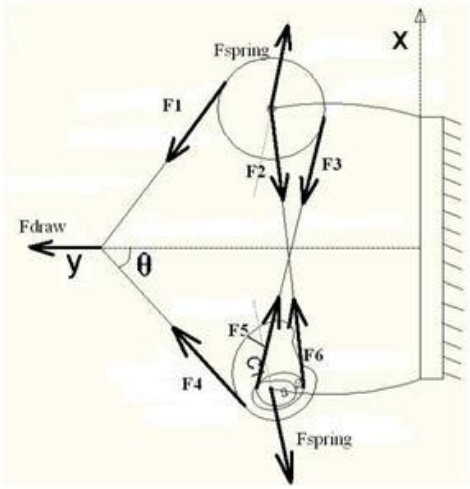

Figure 38 - Force Analysis; Buckmaster BTR

D1, D2, D3, D4, D5, and D6 can be solved using a 2 dimensional point-line distance equation. Referring to Fig.16, ***v*** is perpendicular to the line specified by two points (x_1,y_1) and (x_2,y_2). ***v*** is given by

$$\mathbf{v} = \begin{bmatrix} y_2 - y_1 \\ -(x_2 - x_1) \end{bmatrix}. \qquad (47)$$

The vector **r** is given by

$$\mathbf{r} = \begin{bmatrix} x_1 - x_0 \\ y_1 - y_0 \end{bmatrix}. \qquad (48)$$

Now, by projecting ***r*** onto ***v*** the shortest distance, as well as the moment distance becomes

$$d = \left| \hat{\mathbf{v}} \bullet \mathbf{r} \right| = \frac{\left| (x_2 - x_1)(y_1 - y_0) - (x_1 - x_0)(y_2 - y_1) \right|}{\sqrt{(x_2 - x_1)^2 + (y_2 - y_1)^2}} \qquad (49)$$

In the case of the one cam – one pulley design, the pivot center and the tangent point on the cam constitute ***r***, and the other point that forms the line with the tangent point is the other calculated point on the string. Refer to Figure 13 or 14.

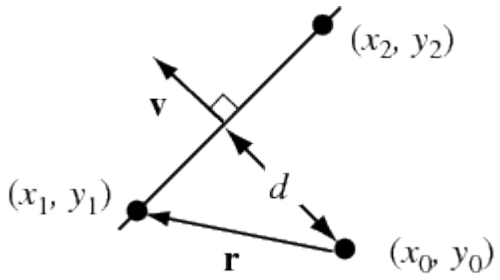

Figure 39 - Point-Line Distance Equation [www.mathworld.wolfram.com,2009]

To solve for Fdraw (Fig.15) the forces acting on the cam and pulley must be solved simultaneously. The limb force, Fspring, is known, since the k-value is assumed to be known. The k- value is related to the direction of tip travel, although the force direction may or may not act along this line. If it does not, the magnitude can be calculated by summing the distance traveled multiplied by the k-value and dividing by the cosine of the angular difference between the assumed limb travel and the actual Fspring direction. The direction of Fspring (both Fspringx and Fspringy) will need to be solved. The equation, however, can be written as:

$$Fspring = \sqrt{Fspringx^2 + Fspringy^2} \qquad (50)$$

Also, since F1 and F4, F2 and F6, and F3 and F5 are along the same cable, they are assumed to be equal. Let us examine the following three equations to extract useful information that will allow Fdraw to be solved for all iterations.

Referring to Fig.15, the following three equations can be formed by kinematically analyzing the stable system.

$$F4 + F5 + F6 + Fspring = 0 \qquad (51)$$

$$T1 = T3 \qquad (52)$$

$$T4 + T5 = T6 \qquad (53)$$

By using Equation 52 and referring to Fig.15, the assumption can be made that F1 and F3 are equal. Since both cables are connected to the same pulley, D1 and D3 are equal, therefore, F1 must be equal to F3. In addition, F4 and F5 are equal. If the forces are broken into their X and Y components and the directions of F4, F5 and F6 are known, then there are only two unknowns.

For example, if we are solving the X component of F4, the Y component of F4 and both X and Y components of F5 are known. Refer to the equations below, where A4 and A5 are angular directions of forces F4 and F5 respectively:

$$F4y = F4x \times \tan(A4), \quad (54)$$

$$F5x = \sqrt{F4x^2 + F4y^2} \times \cos(A5), \quad (55)$$

$$F5y = \sqrt{F4x^2 + F4y^2} \times \sin(A5). \quad (56)$$

Similar to Equation 54, F6y can be solved. Let us next split Equation 58 into its X and Y components. We have:

$$F4x + F5x + F6x + Fspringx = 0 \quad (57)$$

$$F4y + F5y + F6y + Fspringy = 0 \quad (58)$$

Now, by using Equations 50, 54, 57, and 58; F4x, F6x, Fspringx and Fspringy can be solved. The angle, θ, between the y-axis and the force direction of F4 will allow for Fdraw to be solved using Equation 22.

The distance Yh along with the magnitude of Fdraw will allow for a draw-force curve to be plotted. As previously mentioned, this draw-force curve can be used to determine the amount of energy that is stored within the system during a specified draw length. Being able to shoot a fast arrow is directly related to the amount of energy that is stored in the system. In general, A draw-force curve that stores optimal energy will reach the maximum draw force quickly, plateau at a shelf, and reach its holding draw weight over a minimal pulled distance from the maximum draw force. Besides maximizing the amount of stored energy given a set of constraints, efficiency is another important factor to consider to maximize arrow speed. Chapter 4 will discuss how to calculate efficiency for a compound bow and explain where there are efficiency losses in a compound bow.

In Appendix F, numerical results are shown for the first 3 iterations using an excel spreadsheet. More steps can be computed until the holding draw length, Yh, is reached. For this analysis, a limb step size of 0.1 inches is used along the y-axis. The step size along the x-axis is determined by following the limb travel previously defined by (Xl_0,Yl_0) and (Xl_1,Yl_1).

If the results of Appendix F-F3 are compared with Appendix B's measured data we see that both start out along a linear slope. The numerical results of appendix F show that for every inch the force increases linearly about 5.7 pounds. The measured data is comparable at approximately 6.5 pounds per inch. The difference between these results could be a number of various factors. First, the input step size may need to be decreased. Also, the measured cam data may need to be much more precise. For example, the measurement may need to be taken every degree or half degree, and the starting tangent point for each cam may need to be more accurately determined. More accurate cam data will yield a more accurate local equation for equating the slope at each tangent point. Difference in results may also come from human measurement error.

CHAPTER 4

EXPERIMENTAL WORK

4.1 – Determining Efficiency of Compound Bow

For determining the efficiency of a compound bow, two models were tested. The first model tested is a Firestorm Lite by PSE. This model is of the hybrid cam type. The second model tested is a Buckmaster BTR brand bow of the single-cam type. Fig.17 shows both tested bows.

Figure 40 - Buckmaster BTR and PSE Firestorm Lite

The efficiency of a compound bow can be expressed by η; where η is the percentage of work converted to kinetic energy when firing the arrow. Theoretically this value is between $0 < \eta < 1$, but commonly it ranges from 70-85%. If there is conservation of work, then the potential energy would be equal to the kinetic, but there is loss of energy in many parts of the bow due to dynamic conditions. For example, string vibration, limb inertia, arrow stiffness, and cam mass. To find the bow's efficiency we will divide the experimentally determined kinetic energy by the experimentally determined potential energy. Therefore, η equals:

$$\eta = \frac{mv^2}{2\int F(l)dl} \qquad (59)$$

where m is mass, v is velocity, and $\int F(l)dl$ is the force integrated over a pulled distance l.

To determine the kinetic energy experimentally the arrow's weight and the bow's speed were measured. The arrow's weight for both bows tested was 456.6 grains, or 29.57 grams. Speed was measured using a chronograph. An average of five speed tests found the arrows speed to be 231.5 fps with a standard deviation of 0.153 for the Firestorm Lite. These results correspond to a kinetic energy of 73.6 joules. The average speed of the Buckmaster BTR was 220 fps with a standard deviation of 0.308. The amount of kinetic energy produced by this system was 66.5 joules. It should be noted that both bows were not set at IBO standard testing.

To determine the experimental potential energy we first construct a draw-force curve by measuring the amount of force for an incremental draw length. In Fig.15, the bowstring is attached to a fixed scale that measures force. The distance was measured from the front of the arrow shelf to the nock point. The Firestorm Lite had a drawing length of 20 ⅜ inches while the Buckmaster had a drawing length of 20 ⅞ inches. The amount of work stored within the system can be found by integrating the draw-force curve from the brace height to the fully drawn position. An approximation for the work stored, or area under the draw-force curve used, was the average force between two measured forces multiplied by the distance between those points. The force-pounds for each segment were then totaled. A summary of the results found the potential energy of the PSE Firestorm Lite had an ascending (drawn back) work of 813 in-lbs or 92 joules, and a descending (let down) work of 796 in-lbs or 90 joules. The Buckmaster bow had an ascending work of 814 in-lbs or 92 joules, and a descending work of 779 in-lbs or 88 joules.

Figure 41 - Force/Measurement Test taken for PSE Firestorm Lite

The efficiency results were then calculated. The efficiency using the ascending draw-force curve of the PSE Firestorm Lite was 80%. Likewise, the efficiency of the Buckmaster BTR was 72.2%. It can be seen that the amount of work put into both systems are very similar, however since the Firestorm Lite shot faster arrows its efficiency is higher. Results are shown in Appendices B and C.

Through these efficiency tests, there are a few things to note. The first, and most obvious, is that not all bows are created equal. Though arrow speed is probably the biggest design concern, efficiency is also very important and it is directly connected to arrow speed. Greater efficiency allows the archer to produce the most amount of speed with the least amount of effort. Also, efficiency can vary for a given bow for different draw forces. In addition, conclusions can be made to compare overall efficiency for testing various bows, but where efficiency is lost cannot be accurately determined. As previously mentioned, there are many acting components while firing an arrow. The limbs are what store energy in a compound bow. Limb inertia, distance the limbs travel, its speed, and vibration are all connected to the amount of energy that is transferred to the cam. Then, cam rotation itself has a mass moment of inertia and a rotational damping torque between the limb and cam. Also, the bowstring has its own dynamics. There are

vibrations after arrow release, and the string is slightly extensible. The arrow cannot be assumed to be completely rigid either, and it will absorb some energy from the bowstring. All of these dynamics which affect efficiency are beyond the scope of this study, but may need to be considered for future work.

4.2 – Carbon Fiber Bow Limb Manufacturing

Composite materials are good choices for a compound bow limb structure. Composites are much less dense than steel and can carry the same mechanical properties. For example, carbon fiber's density is about five times less than steel and has a slightly higher tensile strength [www.fibreglast.com, 2009]. Also, although steel is much less expensive to manufacture, composite materials are used more often for their thermal expansion properties. The characteristics of steel in 20° F are noticeably different than in 80° F. Carbon fiber and fiberglass composites are much more consistent. These are a few reasons why bow manufacturers use composite limbs on their bows. To understand the manufacturing process, three design experiments were performed.

In these experiments, it was the goal to successfully duplicate a bow limb that has similar properties to bow limbs that are on the market today. A good way to compare two bow limbs is to measure their spring force value; *k*. *k* has units of pounds per inch, for displacement measured at the tip of the limb. In all tests *k* can accurately be assumed as linear. One such bow limb that was used for comparison has a *k* value of 52 pounds per inch.

In a composite material, there is a combination of matrix and fiber that must act in concert to create a structure that yields the properties desired. The matrix material that was chosen for the tests was a two part epoxy resin hardener. It is a medium viscosity, light amber resin that is designed for demanding structural applications. The epoxy resins are the system 2000 series [www.fiberglast.com, 2009]. The fiber material used for the experiments was both unidirectional and plain weave carbon fiber. Since most all of the loading is in one direction, unidirectional fiber is primarily used. A few layers of plain weave were used to prevent cross spliting. For our first and second experiments a foam core was used, because it was thought that very little bending stress would be concentrated near the center bending axis. Other materials that were needed to perform the experiments were: scissors for cutting the fiber, latex gloves and a plastic spoon for applying the epoxy resin to the fiber, a scale and a cup to weigh the epoxy resin mixture, towels, silicone, and plastic sheet for the vacuum bagging process, upper

and lower flat glass surfaces to act as molds, wax to coat the surface of the molds, weights to apply pressure to the molds, and a sander to finish the limb samples.

In the first experiment, two beam samples were made with the same layering structure. Two plain weave (530A), followed by one layer of foam (1022A), then two more plain weave fiber. Cam slots were added. If the results were desirable, then a cam, pin and slot could be easily added. They were compressed using two glass forms coated with soap to prevent adhesion and a plastic sheet that was wrapped around both forms. Towels were twisted and placed around the exterior to create an air channel for the excess air to be vacuumed out. Silicone was placed exterior to the towels to seal air from coming in and out. The purpose of vacuuming out the air is to remove all air bubbles between the layers of fiber that is in the resin. The matrix material used was 0.5 lb of 2000A epoxy, and 0.125lb of 2020A cure agent. Although the cure time for the hardening agent is 20 minutes, more time is need for the part to cure. After one hour the part was taken out, but separated. It was placed in the vacuum longer to cure. Results from the first experiment are shown in Fig.19. When clamped to a vice, it seemed the vice crashed the form. Also, very little bending force would cause the beam to fold and break.

Figure 42 - Carbon Fiber Experiment 1

For the next experiment the following changes will be implemented. It was found that, although the vacuum process worked, it did not work well. If the pump does not keep pumping,

then the air will leak into the bag, loosing air pressure on the glass mold area. Also, it was more time consuming then necessary, since placing a weight above the glass form worked just as well. The amount of resin used was a little too much material, and cure time was too fast. The lump sum heated much faster than the applied portion. It was found the 2060A cure agent worked much better allowing for 60 minutes of cure time compared to 20. Smaller amounts will be used at a time. A parting wax must be used to remove the part from the mold. Soap is cheaper, but not sufficient since the both specimens needed to be heated to in order to part them from the mold. It was also decided for the next experiment to make thicker samples and remove the cam slots. All samples were made without the cam slots, because it was thought that machining cam slots afterward would be easier since sanding and grinding would be required anyway.

For experiment two, three configurations of samples were tested. The following layer structures for the three samples were: sample #1 – 1 plain weave, 1 unidirectional (2583A), 1 foam, 1 unidirectional, and 1 plain; sample #2 – 1 plain weave, 2 unidirectional, 1 foam, 2 unidirectional, and 1 plain weave; sample #3 – 1 plain weave, 6 unidirectional, 1 plain weave, and no foam was used. For the samples, 2 oz of 2000A and 0.5 oz of 2020A hardener was used. Since this is not quite enough for all samples 2 oz of 2000A and 0.5 oz of 2060A was used for the last 3 layers of sample #2 and all of sample #3. Instead of using the vacuum bagging process, the test specimens were weighted down with a brick or piece of steel.

The three samples were removed from their molds 48 hours later. Sample #3 was immediately tested, but folded after only 14 pounds. It seemed the epoxy was not hardened enough at that time. This suspicion turned out to be true. Four days later sample #3 was subject to 20 lb and survived. Sample #1 had permanent deformation at about 8 pounds of lateral loading. Sample #2 was subject to about 16 pounds before permanent deformation. Figs. 20 and 21 show the samples. Fig. 20 shows the three samples after some initial sanding. Sample #3 on the far right show visible signs of damage. In Fig.21 sample #1 and #2 also show deformation.

Figure 43 - Experiment 2; Sample #1, #2, and #3

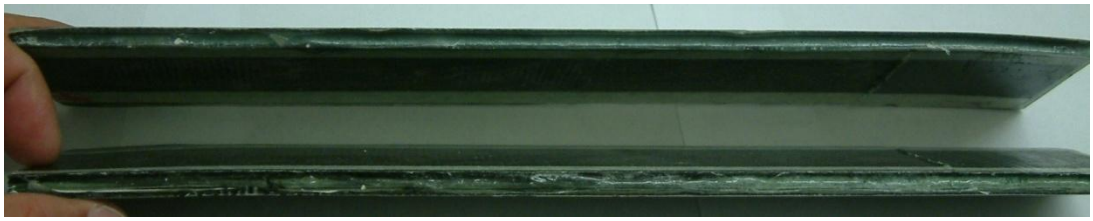

Figure 44 - Experiment 2; Visible Deformation in Sample #1 and #2 with Foam Core

From the above results, it is decided that this type of foam core will not be sufficient. Any amount of compressive stresses will cause the material to collapse. Nomex is a viable option that could be tested for this application; however, it is far more expensive than even carbon fiber and may not be justifiable for cost. Therefore, unidirectional fiber will primarily be used for the third test similar to sample #3, but thicker. A close estimation for the thickness of the new sample can be calculated using the following equation:

$$F = c \times t^3 \qquad (60)$$

Where the transverse loading force, *F*, is equal to the thickness, *t*, cubed multiplied by some constant *c*. Since the force for sample #3 was 20 pounds, and the thickness was 2.7mm, *c* was about 1. We wish to construct a limb that will perform similar to the standard PSE limb with a tested *k* value of 52 pounds per inch. Since the bow limb will deform about three inches the maximum force is about 156 pounds. Thus, the thickness of the new limb will need to be at least

5.4mm. Therefore, by doubling the layers used in sample #3, this will give a close approximation for the maximum allowable force.

For the final experiment, two identical limbs were produced with dimensions of 12 x 2 inches. The layer sequence was: 2 plain weave, 16 unidirectional and 2 more plain weave layers. The limbs were removed from their mold three days later and allowed a week to cure. The thickness of both samples was approximately 5.7 mm or ¼ inch. This is about ⅔ the thickness of the PSE standard limb.

The results were as follows: for a 70 pound pulling force, the sample limb deformed 1.5 inches. Therefore, the *k* value is 46.667 pounds per inch, which is very similar to the tested limb (52 lbs/in). There was no permanent deformation. A similar PSE limb was found to be made of unidirectional fiberglass composite. It was almost translucent after the paint was sanded off. Figure 22 shows the unsanded sample of the carbon fiber limbs and Figure 23 shows the sanded sample. It is not necessary to have a glossy finish, since the limb will most likely be painted to protect it from environment conditions.

Figure 45 – Experiment 3 Before Surface Post-processing (Sanding, Polishing)

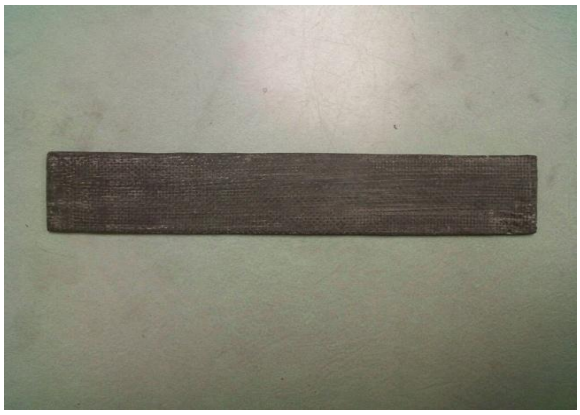

Figure 46 - Experiment 3; Sanded Sample of 2 Plain, 16 Unidirectional, 2 Plain

It can be concluded from the following experiments that a successful process for manufacturing a composite bow limb structure was shown. One can now know the materials that are necessary to construct a limb, an approximate number of carbon fiber layers, and a similar width and length dimension to produce a workable limb. Other considerations are a slot for the cam and also a pin connection for the cam to connect to the limb. If there is a greater volume of limbs being manufactured with the same dimensions, it may be useful to create a mold for the unidirectional fiber layers to be placed in. This will allow the tolerances of the final product to be much more consistent.

CHAPTER 5

CONCLUSION AND FUTURE WORK

It has been shown that most patented compound bow designs came about empirically. Through this study, compound bows were more thoroughly examined by an analytical approach. More specifically, the twin symmetric and single cam designs were analyzed. The main objective of designing a top performing compound bow is to shoot fast arrows with accuracy. As stated in Chapter 1, there are certain constraints known as IBO standards and those set in place by the industry and consumer demand that must be followed. One of the biggest design characteristics that affect arrow speed is cam geometry. Another is efficiency of the system (Chapter 4).

Cam geometry, limb geometry and limb properties are directly related to the amount of stored energy that can be achieved within the draw length. This draw-force curve is more commonly known as the let-off curve for compound bows. By changing the cam geometry, limb or both a different let-off curve is formed. If the only objective is maximum arrow speed, then a desirable let-off curve maximizes the amount of stored energy in a given draw distance. This correlates to a curve that reaches its maximum draw weight within a minimal pulled distance and also reaches its holding draw weight in a minimal pulled distance. A desirable let-off curve will have something characteristic of a shelf at peak draw weight.

The analytical model discussed in Chapters 3 and 4 can successfully form a let-off curve from known cam and limb geometries and initial conditions using an iterative approach for both Twin Symmetric and Single Cam designs. Appendix F shows three iterations for a single cam design. As discussed in Chapter 3, after reviewing the numerical results, measurement of cam and limb geometries as well as initial conditions need to be very accurate and precise if existing bows are being measured.

Referring to the compound bow analysis, for future work, an optimization tool should be formed. For example, if a designer wishes to create a bow with a 70 lb. maximum draw weight, 30 in. draw length, 7 in. brace height, and 70% let-off; along with 12 inch limbs and an axle to axle length of 30 inches, they should be able to find a maximized let-off curve that meets these requirements.

Another important issue in designing a compound bow is efficiency. As discussed in Chapter 4, efficiency loss comes from various parts of the bow. For example, string vibration, limb inertia, arrow stiffness, and cam mass all contribute to efficiency loss. In Chapter 4, tests to determine overall efficiency have been performed. Steps have already been taken to determine

individual efficiency loss; however, the entire work has not yet been pieced together. Conservation of energy is used to do the analysis and using calculus of variation the energy equation can be derived. The dynamic system can be solved using central difference method.

If individual cause of efficiency loss is known, efforts can be directed towards areas of greater losses. Also, if these efficiency results were integrated with the previously mentioned optimization tool, a theoretical bow model will have been formed. If a robust software tool could be successfully implemented, this would save manufacturer's time and money in research and prototyping costs. But, as one can see, there is much work still to be done.

REFERENCES

Allen, H. W., 1968, Archery Bow with Draw Force Multiplying Attachments, US Patent No.3486495.

Blahnik, R. C., 2006, Compound Bow with Adjustable Let-off, US Patent No.7059315 B2.

BowTech, 2009 :: Refuse to Follow. , 2009, <http://www.bowtecharchery.com/downloads/EqualizerSystem.pdf>.

Blanton, M., 2007, "2007 Compound Bow Specification Database & Comparison Charts." 24 Feb. 2009 <http:www.huntersfriend.com>.

Darlington, R. F., 2000, Single-Cam Compound Archery Bow, US Patent No.6082347.

International Bowhunting Organization, "IBO Rules Class Definitions.", 2009, <http://www.ibo.net/>.

Ketchum, F. W., 1976, Compound Bow, U.S. Patent No.3958551

Kincy, M. A., 1981, "A Model for Optimization of the Archer's Compound Bow." Thesis. University of Missouri – Rolla.

Knittel, J., 2008, (Engineering Director, Concept Archery Corp.), personal correspondence.

Kudlacek, D. S., 1977, Compound Archery Bow with Eccentric Cam Elements, US Patent No.4060066.

Lin, Y. and Hanson, A., 2008, Analysis and Design of a Class of Cam Profile, *International Mechanisms and Machine Science Conference,* Dalian, China.

McPherson, M. A., 1994, Dual-feed Single Cam Compound Bow. Bear Archery Inc., assignee. Patent No.5368006.

Miller, L., 1996, Single Cam Compound Bow, US Patent No.5505185.

"Physical Properties of Laminates - Fibre Glast Developments." Fiberglass, Carbon Fiber - Fibre Glast Developments Corp., 2009, <http://www.fibreglast.com/>.

Strother, K. D., 1998, Efficient Power Cam for a Compound Bow, US Patent 5975067.

Visnor, J. C., 2007, "Analytical and Experimental Analysis of the Large Deflection of a Cantilever Beam Subjected to a Constant, Concentrated Force, With a Constant Angle, Applied at the Free End." Thesis. University of Akron.

Wolfram MathWorld: The Web's Most Extensive Mathematics Resource. 2009 <http://mathworld.wolfram.com/Point-LineDistance2-Dimensional.html>.

APPENDICES

APPENDIX A – PARTIAL LIST OF COMPOUND BOW MANUFACTURERS

BRAND NAME	WEBSITE	AVERAGE COMPOUND BOW SPEED (FPS) *
Alpine	www.alpinearchery.com	310.5
APA	www.apaarchery.com	327.5
Archery Research	www.archeryresearch.com	311.5
Bow Zone	www.bowzonearchery.com	310
Bowtech	www.bowtecharchery.com	324.2
Browning	www.browning-archery.com	306.8
Concept Archery	www.conceptarchery.com	312
CSS	Phone : (314) 781 – 3945	298.4
Darton	www.dartonarchery.com	310.1
Diamond	www.diamondarchery.com	310.6
Evotek	www.evotekbows.com	313.3
Fred Bear	www.beararcheryproducts.com	308.5
Hoyt	www.hoyt.com	301.5
Kodiak	www.kodiak-archery.com	306.2
Martin	www.martinarchery.com	310.7
Matthews	www.matthewsinc.com	314
Parker	www.parkerbows.com	306.9
Pearson	www.benpearson.com	313.2
PSE	www.pse-archery.com	304.7
Reflex	www.reflexbow.com	302.8
Ross	Division of Bowtech	308.3
Rytera	www.rytera.com	312.5
Whisper Creek	www.whispercreekarchery.com	307.8

* 2007 Compound Bow Specification Database & Comparison Charts Results from www.Huntersfriend.com. Bow speed is calculated at a 30 inch draw with 5 grain arrow for every pound of maximum draw (*example – 70# maximum draw will shoot a 350 grain arrow*).
** This is not a comprehensive list of all bow manufacturers.

APPENDIX B – FIRESTORM LITE EFFICENCY DATA

Potential Energy (Draw Force Curve)				
Draw Length	**Ascending force (lbs)**	average force * draw length	**Descending Force (lbs)**	average force * draw length
10 5/8	0	5/8	0	3/4
11	3.3	6 2/3	4	8
12	10	14	11.9	15 4/5
13	18	22 1/2	19.7	23 3/5
14	27	31 1/4	27.5	31 1/2
15	35.5	39 5/9	35.5	38 8/9
16	43.6	46 2/3	42.3	45 4/5
17	49.7	51 1/2	49.3	51 1/2
18	53.3	54 3/4	53.7	53 2/3
19	56.2	55 6/7	53.6	53
20	55.5	54 1/7	52.2	51 4/5
21	52.8	52	51.4	50 5/7
22	51.3	51 1/2	50	50 2/7
23	51.7	51 2/3	50.6	50 2/7
24	51.6	51 1/2	50	50 1/9
25	51.4	51	50.2	50
26	50.6	49	49.7	47 2/3
27	47.2	43 3/4	45.6	43
28	40.3	36 3/4	40.3	35 2/7
29	33.2	28 1/3	30.3	26 1/9
30	23.4	20 1/2	21.9	19
31	17.6		16	
Total (lbs*in)		813 3/8		796 4/9
joules >>>		91.932		89.986

Kinetic Energy		
Velocity (m/s)		**Arrow Mass (grams)**
70.56		29.57
70.79		
70.55		**Std. Dev.**
70.36		0.153199217
70.6		
average>>>	70.57	approx. 231.5 fps
Kinetic Energy (joules)		
73.635		

Efficiency - η	
ascending	80.1%
descending	81.8%

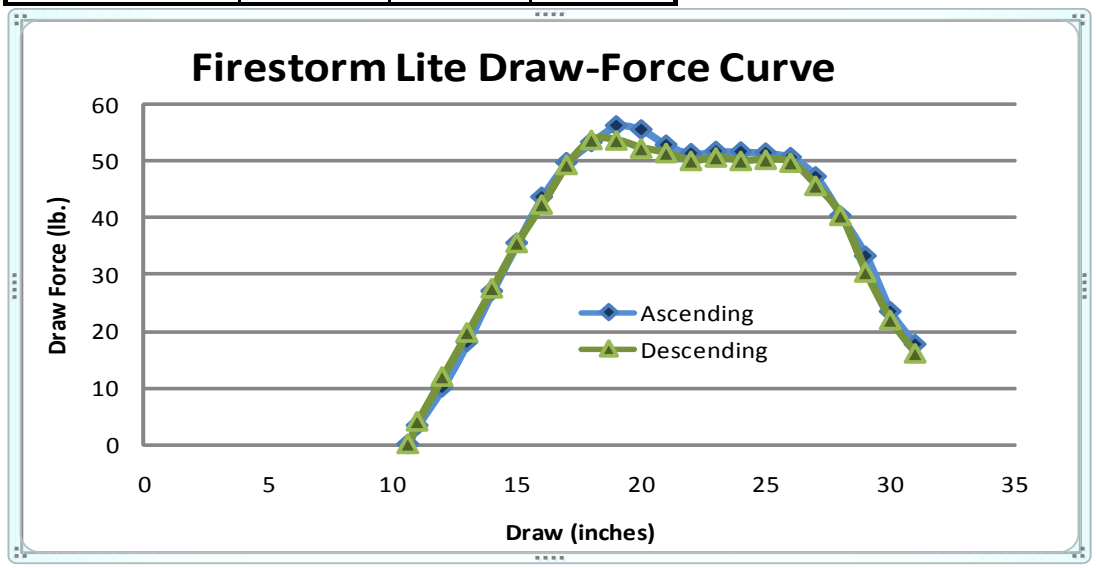

APPENDIX C – BUCKMASTER BTR EFFICIENCY DATA

Potential Energy (Draw Force Curve)				
Draw Length	Ascending force (lbs)	average force * draw length	Descending force (lbs)	average force * draw length
9 1/8	0	2.1875	0	2.23125
10	5	9	5.1	8.35
11	13	15.6	11.6	14.4
12	18.2	21.6	17.2	20.5
13	25	28.25	23.8	26.9
14	31.5	33.95	30	32.5
15	36.4	39	35	38.15
16	41.6	44.4	41.3	43.15
17	47.2	49.2	45	47.5
18	51.2	52.6	50	50.05
19	54	54.5	50.1	50.55
20	55	55	51	51.25
21	55	55.5	51.5	51.45
22	56	55.1	51.4	52.3
23	54.2	54.45	53.2	53.2
24	54.7	52.1	53.2	50.85
25	49.5	47.95	48.5	47.25
26	46.4	46.05	46	45
27	45.7	42.35	44	38.95
28	39	32.9	33.9	30.65
29	26.8	22.9	27.4	23.65
30	19		19.9	
Total (lbs*in)		814.5875		778.83125
joules >>>		92.04		88

Kinetic Energy		
Velocity (m/s)		Arrow Mass (grams)
67.24		29.57
67.03		
66.56		std. dev.
67.25		0.308334234
67.31		
average>>>	67.078	approx. 220 fps
Kinetic Energy (joules)		
66.52449		

Efficiency - η	
ascending	72.3%
descending	75.6%

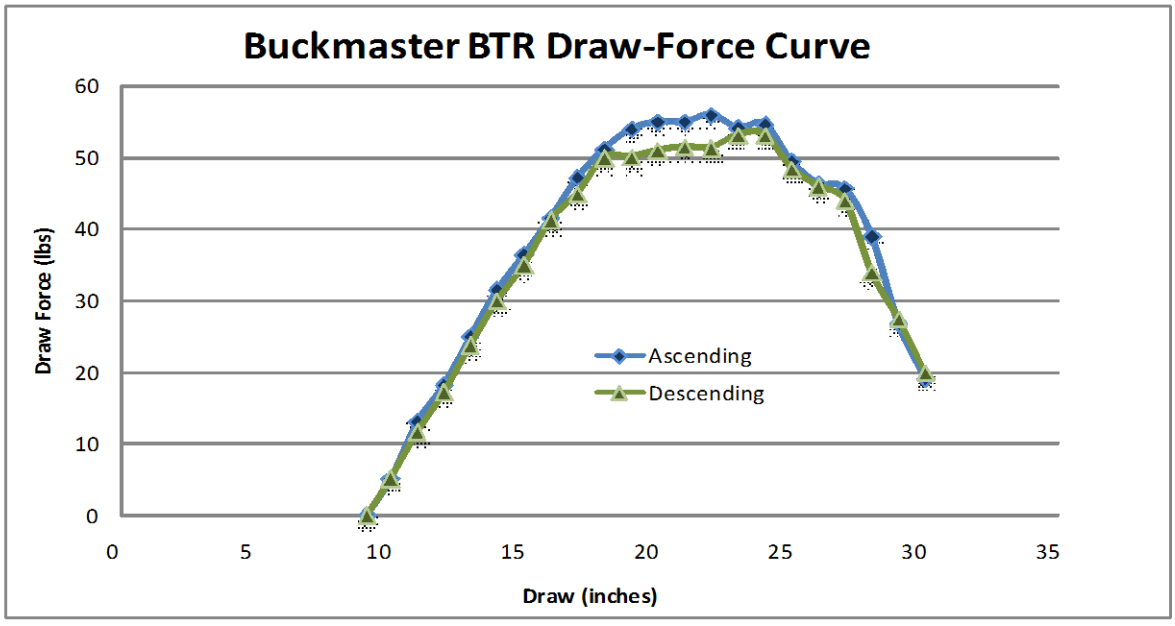

APPENDIX D – TOOLS AND PRODUCTS USED IN EXPERIMENTAL WORK

Tool or Product	Model # or Part #	Manufacturer/Location

Tools Used for Efficiency Experiments

Compound Bow	Buckmaster BTR	Bear Archery / Gainesville, Florida
Compound Bow	Firestorm Lite	PSE – Archery / Tucson, Arizona
Arrow	Carbon Fury 6075	Redhead Bass Pro Shops Springfield, Missouri
Chronograph	M-1	Shooting Chrony Inc./ Mississauga, Ontario
Electronic Scale	iBAL 201	My Weigh GKI Technologies/ Las Vegas, Nevada
Hanging Scale	Electro Samson 75593	Salter Brecknell/ Avery Weigh-Tronix Fairmont, Minnesota
Other Tools Used: Archery Target, Tape Measure, Mechanical Arrow Release, Vice for mounting hanging scale		

Tools and Products Used for Limb Manufacturing

Electronic Scale	iBAL 201	My Weigh GKI Technologies/ Las Vegas, Nevada
Release Wax	Partall Paste #2; #1016-A	Rexco/ Conyers, Georgia
20 Minute Epoxy Cure	2020	Fibre Glast Developments Corp./ Brookville, Ohio
60 Minute Epoxy Cure	2060	Fibre Glast Developments Corp./ Brookville, Ohio
Epoxy Resin	2000	Fibre Glast Developments Corp./ Brookville, Ohio
PVA Release Film	13	Fibre Glast Developments Corp./ Brookville, Ohio
Other Tools Used: Latex gloves, paper towels, glass forms, vacuum pump, plastic sheeting, epoxy resin applicator		

APPENDIX E – BUCKMASTER BTR MEASURED CAM PROFILE

E1 – SINGLE CAM (C1 BOTTOM, C2 MIDDLE, C3 TOP) *Note – theta starts at first tangent point where bow cable comes in contact with cam. Distance is measured from rotational center to cam edge. Measurements are taken in direction of rotation (counterclockwise in picture).

E2 – C1 CAM DATA

C1	
Theta (degrees)	Distance (mm)
0	0.288
5	0.576
10	1.152
15	2.304
20	3.456
25	5.76
30	9.216
35	13.248
40	16.704
45	23.616
50	28.224
55	33.408
60	38.592
65	43.2
70	48.384

75	52.992
80	57.024
85	60.48
90	63.36
95	65.664
100	67.968
105	69.696
110	70.272
115	70.848
120	70.848
125	70.272
130	69.696
135	68.544
140	67.968
145	66.816
150	65.664
155	63.936
160	62.784
165	60.48
170	58.752
175	57.024
180	54.72
185	51.264
190	41.472
195	38.592
200	33.984
205	28.224
210	22.464
215	16.704
220	8.64
225	5.184
230	4.608
235	4.032
240	3.456
245	2.88
250	2.88
255	2.88
260	2.88
265	2.88
270	2.88
275	2.88
280	2.88
285	2.88
290	2.88
295	2.88
300	2.88
305	2.88
310	2.88
315	2.88

320	2.88
325	2.88
330	2.88
335	2.88
340	2.88
345	2.88
350	2.88
355	2.88
360	2.88
365	2.88
370	2.88
375	2.88
375	2.88

E3 – C2 CAM DATA, +110 DEGREES RELATIVE TO C1 IN DIRECTION OF ROTATION

C2	
Theta (degrees)	Distance (mm)
0	57.024
5	56.448
10	56.448
15	56.448
20	55.872
25	55.872
30	55.296
35	54.144
40	51.84
45	49.536
50	47.808
55	45.504
60	43.776
65	42.048
70	40.896
75	39.744
80	38.592
85	36.864
90	35.136
95	32.832
100	31.104
105	28.224
110	25.92
115	23.616
120	20.736
125	17.856
130	14.976
135	12.096
140	9.216
145	8.064
150	6.912

155	6.336
160	6.336
165	5.76
170	5.184
175	5.184
180	4.608
185	4.608
190	4.032
195	4.032
200	4.032
205	4.032
210	4.032
215	4.032
220	4.032
225	4.032
230	4.032
235	4.608
240	5.184
245	5.184
250	5.76
255	6.336
260	6.912
265	8.064
270	9.216
275	9.792
280	10.368
285	11.52
290	13.824
295	14.976
300	17.856
305	20.16
310	23.04
315	28.224
320	31.68
325	36.864

E4 – C3 CAM DATA, -20 DEGREES RELATIVE TO C1 IN DIRECTION OF ROTATION

C3	
Theta (degrees)	Distance (mm)
0	5.76
5	5.184
10	5.184
15	5.184
20	5.184
25	5.184
30	5.184
35	5.184
40	5.184

45	5.184
50	5.184
55	5.184
60	5.184
65	5.76
70	5.76
75	5.76
80	6.336
85	6.336
90	6.912
95	6.912
100	8.064
105	8.64
110	9.216
115	9.216
120	10.368
125	11.52
130	13.248
135	14.976
140	17.28
145	20.736
150	23.04
155	27.072
160	30.528
165	34.56
170	39.168
175	42.624
180	46.08
185	48.384
190	50.688
195	52.416
200	53.568
205	54.144
210	54.72
215	54.144
220	53.568
225	52.992
230	51.84
235	48.384
240	46.656
245	43.2
250	40.896
255	35.712

APPENDIX F – BUCKMASTER BTR NUMERICAL RESULTS USING MICROSOFT EXCEL

F1 – CALCULATED RESULTS

Iteration 1		Subiteration 1 (translation)		Iteration 2 (rotation)		Subiteration 2 (translation)		Iteration 3 (rotation)		
Input Variables										
Yc	-8.5		-8.6		-8.6		-8.7		-8.7	
Xc	16.4375		16.2105		16.2105		15.9835		15.9835	
(-Xc)	-16.4375		-16.2105		-16.2105		-15.9835		-15.9835	
Initial Variables										
Yp10	-7.155137158	Yp11	-7.255137158	Yp12	-7.253344101	Yp13	-7.353344101	Yp14	-7.400446701	
Xp10	-16.31983975	Xp11	-16.54683975	Xp12	-16.14786285	Xp13	-15.92086285	Xp14	-15.91837335	
Yp20	-9.85	Yp21	-9.95	Yp22	-8.733539671	Yp23	-8.833539671	Yp24	-8.955183931	
Xp20	-16.4375	Xp21	-16.6645	Xp22	-14.86712582	Xp23	-14.64012582	Xp24	-14.65783746	
Yh0	-9.85			Yh1	-10.78566935	avg		Yh2	-12.00091987	avg
				Yh1(cam side)	-10.69095727	-10.73831331		Yh2 (cam side)	-11.94281691	-11.971868
Yt10	-8.511338583	Yt11	-8.611338583	Yt12	-7.909040245	Yt13	-8.009040245	Yt14	-8.057183224	
Xt10	16.4375	Xt11	16.2105	Xt12	16.26133022	Xt13	16.03433022	Xt14	16.03345851	
Yt20	-6.25496063	Yt21	-6.35496063	Yt22	-7.043975602	Yt23	-7.143975602	Yt24	-7.007343058	
Xt20	16.4375	Xt21	16.2105	Xt22	16.40255109	Xt23	16.17555109	Xt24	16.18566307	
Yt30	-8.273228346	Yt31	-8.373228346	Yt32	-8.768320377	Yt33	-8.868320377	Yt34	-9.00996724	
Xt30	16.4375	Xt31	16.2105	Xt32	16.42367839	Xt33	16.19667839	Xt34	16.19789463	

F2 – FORCE RESULTS

	Iteration 2	Iteration 3
D4	0.672020137	0.612878256
D5	0.158233898	0.298847709
D6	1.54510367	1.679696066
F1 (direction)	-0.00898197	-0.01740763
F2 (direction)	0.047675554	0.052568898
F3 (direction)	-0.046478771	-0.05007354
F4 (direction)	3.184058083	3.181663402
F5 (direction)	3.095113883	3.091519118
F6 (direction)	3.189268208	3.194161551
F4&F5 (dir.)	3.139585983	3.13659126
Fspring(dir.)	-0.011684195	-0.01516169
Fspring(limbdir.)	0.414949679	0.414949679
Fspring(difference)	0.426633874	0.430111369
F4X (LBS)	-28.09722615	-33.6673411
F4Y (LBS)	-1.193878497	-1.34979809
F4 (LBS)	28.12257924	33.69438843
F5X (LBS)	-28.09220844	-33.6521553
F5Y (LBS)	1.306632346	1.686492189
F6X (LBS)	-15.09436218	-18.2637871
F6Y (LBS)	0.720177814	0.96099255
Fspring (lbs)	64.8986207	77.7972414
FspringTOT(lbs)	71.2886629	85.5931213
FspringX (lbs)	71.28379677	85.58328351
FspringY (lbs)	-0.832931662	-1.29768665
Fdraw (lbs)	4.917065266	12.09837509

F3 – FIRST THREE DRAW FORCE CURVE POINTS

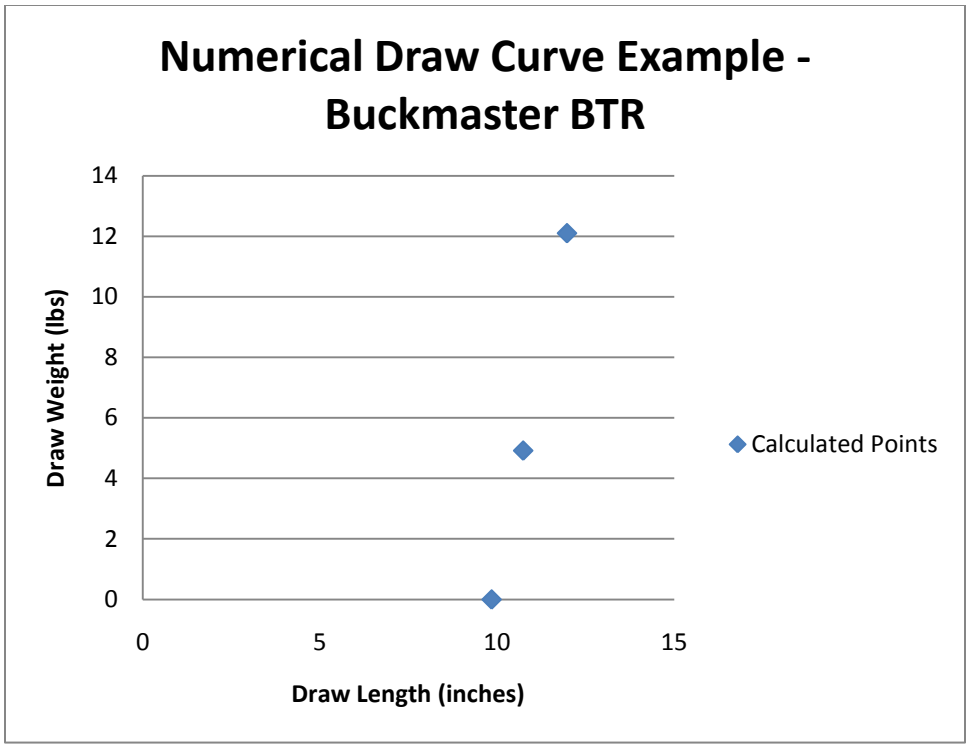
Numerical Draw Curve Example - Buckmaster BTR
Draw Weight (lbs)
14
12
10
8
6
4
2
0
0
5
10
15
Draw Length (inches)
Calculated Points